

Rolling motion of non-axisymmetric cylinders

Antonino Carnevali^a

Department of Physical Sciences, Morehead State University, UPO 715, Morehead, Kentucky 40351-1689

Russell May^b

Department of Mathematics and Computer Science, Morehead State University, UPO Box 701, Morehead, Kentucky 40351-1689

(Received 12 November 2004; accepted 4 July 2005)

Theoretical and experimental results are compared for the rolling motion of cylinders on a ramp. An asymmetric distribution of the mass makes the motion jerky and complex and is an interesting and simple example of Lagrangian mechanics. © 2005 American Association of Physics Teachers.

[DOI: 10.1119/1.2008298]

I. INTRODUCTION

The “Great Soup Can Race” is frequently used as a challenge for high school science teams participating in Science Olympiads and as an illustration of the application of basic physics principles. Students are given various materials to build a cylindrical can that will win the race to the bottom of a ramp. In general, the lesson is intended to be that the system acquiring less rotational energy will have greater translational energy and will therefore win the race. Accordingly, the underlying assumption is that the smaller the moment of inertia—for a given mass added to the can—the faster the can. Although this conclusion is correct for symmetric systems, it is incorrect in general. A non-axisymmetric distribution of the additional mass changes the initial potential energy and the torque distribution and, under proper conditions, produces the fastest system. Additionally, the motion of non-axisymmetric cylinders is varied and interesting to view, and the corresponding theory is solvable for the case of rotation without slipping. Thus, this system would make an excellent project for undergraduate students who have had Lagrangian mechanics.

II. ANALYSIS

The soup can is a hollow cylinder of radii R_1 and R_2 and mass m (see Fig. 1 for the definition of the other quantities). For rolling without slipping, we have

$$x = R_2(\phi - \phi_0). \quad (1)$$

The added mass is a rod of radius r and mass M , parallel to the axis of the hollow cylinder, and located at a distance R from its axis. The center of mass of the system with respect to this axis is at

$$R_{c.m.} = \frac{MR}{m+M}. \quad (2)$$

We can use Lagrange’s equations^{1,2} to determine the equation for the linear acceleration of the system down the ramp. The potential energy is

$$U = (m+M)gh_{c.m.} = (m+M)g[(L-x)\sin(\gamma) + R_2 \cos(\gamma) - R_{c.m.} \cos(\gamma + \phi)], \quad (3)$$

and the kinetic energy is³

$$T = T_{c.m.} + T', \quad (4)$$

where $T_{c.m.}$ is the kinetic energy of the total mass moving with the velocity of the center of mass and T' is the kinetic energy of the individual components relative to the center of mass. Thus,

$$\begin{aligned} T_{c.m.} &= \frac{1}{2}(m+M)(\dot{x}_{c.m.}^2 + \dot{y}_{c.m.}^2) \\ &= \frac{1}{2}(m+M)[\dot{x}^2 + R_{c.m.}^2 \dot{\phi}^2 - 2R_{c.m.} \cos(\phi)\dot{x}\dot{\phi}], \end{aligned} \quad (5)$$

and

$$T' = T'_{cyl} + T'_M. \quad (6)$$

The two parts of T' are

$$T'_{cyl} = \frac{1}{2}I\dot{\phi}^2, \quad (7)$$

where the moment of inertia I is about the axis passing through the center of mass of the system. Thus,

$$I = I_0 + mR_{c.m.}^2, \quad (8)$$

where I_0 is the moment of inertia of the cylinder about its own axis. Hence

$$T'_{cyl} = \frac{m}{2} \left[\frac{R_1^2 + R_2^2}{2} + R_{c.m.}^2 \right] \dot{\phi}^2, \quad (9)$$

and

$$T'_M = T'_{rev} + T'_{spin} \quad (10a)$$

$$= \frac{1}{2}(I_{revolution} + I_{spin})\dot{\phi}^2 \quad (10b)$$

$$= \frac{M}{2} \left[(R - R_{c.m.})^2 + \frac{r^2}{2} \right] \dot{\phi}^2. \quad (10c)$$

If we substitute Eqs. (2), (9), and (10c) into Eq. (6) and simplify, we obtain

$$T' = \frac{1}{2} \left[m \left(\frac{R_1^2 + R_2^2}{2} \right) + \mu R^2 + \frac{Mr^2}{2} \right] \dot{\phi}^2, \quad (11)$$

where the reduced mass is

$$\mu = \frac{mM}{m+M}. \quad (12)$$

The total kinetic energy of the system is therefore

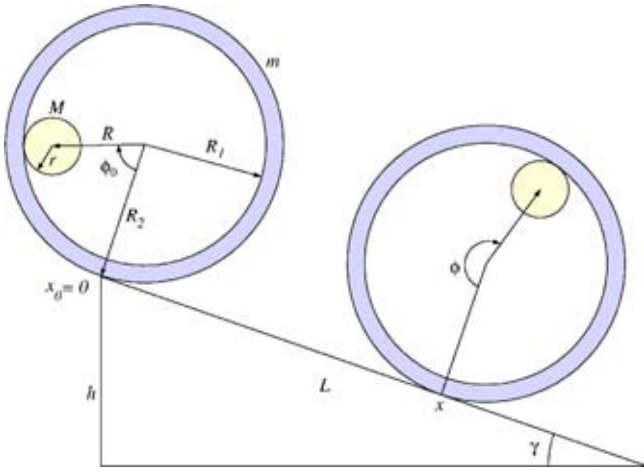


Fig. 1. A rolling asymmetric cylinder on a ramp with length L and angle of inclination γ . A rod of mass M is fixed on the cylinder at a radial distance R and initially located at the angle ϕ_0 from the normal to the ramp. As the cylinder rolls distance x down the ramp, M rotates to the angular position ϕ .

$$T = \frac{1}{2}(m + M)[\dot{x}^2 + R_{c.m.}^2 \dot{\phi}^2 - 2R_{c.m.} \cos(\phi) \dot{x} \dot{\phi}] + \frac{1}{2} \left[m \left(\frac{R_1^2 + R_2^2}{2} \right) + \mu R^2 + \frac{Mr^2}{2} \right] \dot{\phi}^2. \quad (13)$$

The same result is obtained by starting from $T = T_{cyl} + T_M$ instead of $T = T_{c.m.} + T'$. The Lagrangian of the system is

$$\mathcal{L} = \frac{1}{2}(m + M)(\dot{x}^2 + R_{c.m.}^2 \dot{\phi}^2 - 2R_{c.m.} \cos(\phi) \dot{x} \dot{\phi}) + \frac{1}{2} \left[m \left(\frac{R_1^2 + R_2^2}{2} \right) + \mu R^2 + \frac{Mr^2}{2} \right] \dot{\phi}^2 - (m + M)g[(L - x)\sin(\gamma) + R_2 \cos(\gamma) - R_{CM} \cos(\gamma + \phi)]. \quad (14)$$

The Lagrangian can easily be changed from $\mathcal{L}(x, \phi, \dot{x}, \dot{\phi})$ to $\mathcal{L}(x, \dot{x})$ using Eq. (1):

$$\mathcal{L} = \frac{\dot{x}^2}{2R_2^2} \left[(m + M)R_2^2 + MR^2 - 2MRR_2 \cos\left(\phi_0 + \frac{x}{R_2}\right) + \frac{m}{2}(R_1^2 + R_2^2) + \frac{Mr^2}{2} \right] + (m + M)g \left[x \sin(\gamma) + R_{c.m.} \cos\left(\gamma + \phi_0 + \frac{x}{R_2}\right) \right] + \text{constant}. \quad (15)$$

Finally, Lagrange's equation yields the linear acceleration of the system down the ramp

$$\ddot{x} = \frac{(m + M)gR_2^2 \sin(\gamma) - MgRR_2 \sin(\gamma + \phi) - MR \sin(\phi)\dot{x}^2}{MR^2 + (m + M)R_2^2 + \frac{m}{2}(R_1^2 + R_2^2) + \frac{Mr^2}{2} - 2MRR_2 \cos(\phi)}. \quad (16)$$

We have chosen to solve Eq. (16) in terms of \dot{x} and \ddot{x} , instead of $\dot{\phi}$ and $\ddot{\phi}$, because our measurements give $\dot{x}(t)$. As a check, Eq. (16) reduces to the simple analytical results⁴ for symmetric cases, that is, for $M=0$ or for $R=0$, including the case $r=R_1$, that is, a solid cylinder. In general, Eq. (16) is

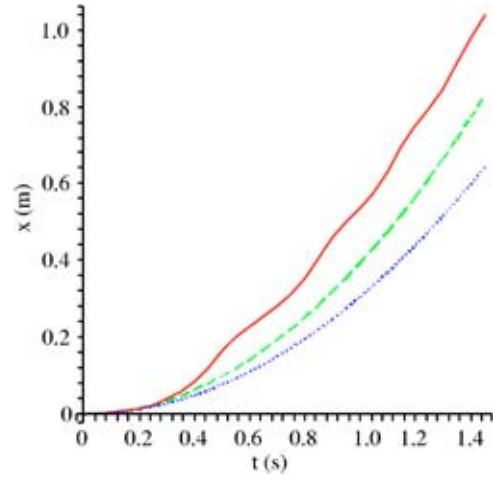


Fig. 2. Calculation of the positions of three cylinders rolling down a 15° ramp. The dotted line represents the motion of an empty cylinder, the dashed line a cylinder with additional mass M on its axis, and the solid line a cylinder with M at its edge. The following parameters (matching an experimental run) were used: $m=230$ g, $M=255$ g, $R_1=3.8$ cm, $R_2=4.4$ cm, $R=2.6$ cm, and $r=1.0$ cm.

nonlinear, so the motion can only be computed numerically. For the general, non-axisymmetric case, we used a fourth-order Runge-Kutta algorithm to compute the motion of the cylinder by converting Eq. (16) to a pair of first-order equations, $\dot{x}=v$ and $\dot{v}=g(x,v)$ where g is the right-hand side of Eq. (16) with ϕ replaced by $x/R_2 + \phi_0$ and \dot{x} replaced by v .

III. MOTION DOWN THE RAMP

With ϕ_0 appropriately large ($\approx 200^\circ$) and M located as far as possible from the axis, it is easy to test experimentally that the non-axisymmetric cylinder wins the race. Figure 2 shows the results for three configurations: an empty cylinder, a cylinder with additional mass M on its axis, and a cylinder with M placed at its edge. Not shown in Fig. 2 is the general result that the symmetric cylinder (with M on the axis) will eventually win the race if the ramp is long enough due to the fact that the rotational energy keeps increasing, whereas the additional initial potential energy of the non-axisymmetric cylinder is constant.

To compare the predictions of the simulation with data collected with a motion detector, we plotted the translational velocity rather than the distance, because the variations in the former are more dramatic and a better visual test of the theory. We used two simple systems. One is a short PVC pipe with a large bolt and nut used as the eccentric mass M , with $M \approx m$. The other is an empty, large coffee can, with both ends removed, and a 1 kg rod used as the eccentric mass, so that $M \gg m$. Elastic bands on the outer rims were used to prevent slipping. The largest experimental uncertainties were the frictional losses, which were not systematically measured, but included in an ad hoc manner in the model as discussed in the following, and the precision of the measurement of ϕ_0 of only $\pm 1^\circ$. There also was significant uncertainty in the starting time for cases such as that of Fig. 3, where the system is initially close to equilibrium [$\phi_0=180^\circ$ and $\phi_{\text{equil}}=163^\circ$ from Eq. (19)]. Generally, a smaller time uncertainty $\Delta t \approx 0.04$ s is due to the fact that the cylinder is released by hand and the data acquisition rate is ≈ 40 Hz.

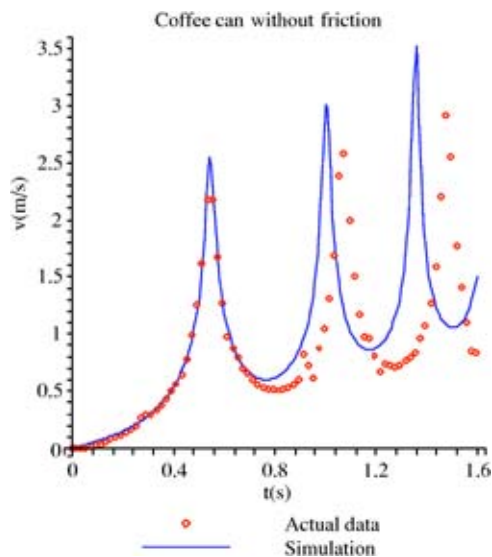


Fig. 3. The following experimental values were used in the calculation: $\gamma = 6.75^\circ$, $\phi_0 = 180^\circ$, $m = 195$ g, $M = 1000$ g, $R_2 = 7.7$ cm, $R_1 = 7.6$ cm, $R = 6$ cm, and $r = 1.25$ cm.

Figure 3 shows the results for $M \gg m$, a case that enhances the jerky motion of the system. Measurements of the distance traveled and number of rotations show that the slipping was minimal. However, the motion in this case was unsteady and the ramp was visibly shaking. Some kinetic energy was obviously lost by the can in this process. Additional energy was lost because of air resistance as well as deformations at the contact point. For the PVC pipe system, which experienced smaller losses due to its smoother motion, we estimated the total energy lost during several runs by measuring ϕ_0 and ϕ and \dot{x} at a convenient point down the ramp. This point was chosen to be the last local minimum of v because there the angle was ϕ_{equil} , which is easy to determine and is given in Eq. (19). Our results show that $\Delta E/E \approx 5\%$ at low speeds, then increases sharply as the average rotational frequency approached 3 rev/s. At 3.5 rev/s, $\Delta E/E \approx 20\%$. Energy losses for the coffee can system are expected to be larger.

Good agreement between theory and experiment can be expected only if frictional losses are taken into account. We accounted for frictional losses by introducing an empirical frictional acceleration, a_f , in addition to the acceleration in Eq. (16). Air drag would contribute a small term proportional to v^2 , while the rolling resistance would add a constant term plus a term proportional to v at higher speeds, or a term proportional to $v^{2.5}$ at very high speeds⁵ higher than those encountered in this experiment. Vibrational losses to the ramp and other losses cannot be easily quantified. For simplicity, we used an ad hoc approach and assumed simple forms for a_f in the following comparisons. Figure 4 shows excellent agreement between theory and experiment when $a_f \propto v^2$ is assumed.

Figure 5 shows a similar comparison for motion down the ramp of the PVC pipe system, with $M \approx m$. Excellent agreement is obtained with $a_f \propto v$. We note that rolling resistance at very low velocities (< 0.5 m/s) results in a constant a_f term.⁵⁻⁷ If we apply the methods of Ref. 7 to our two systems, we find $a_f \approx 0.06$ m/s² for both cylinders. The average value of a_f calculated for the coffee can simulation of Fig. 4

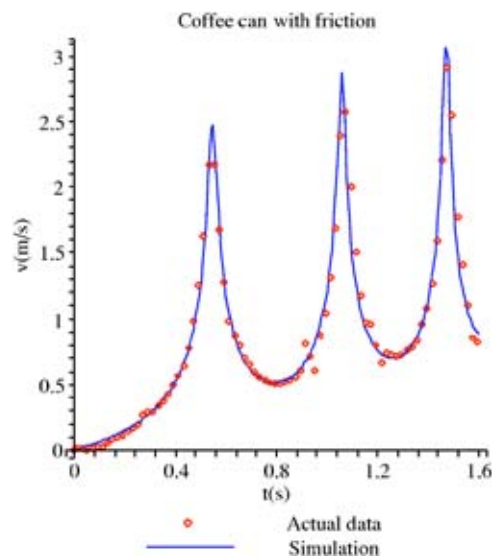


Fig. 4. Same parameters as Fig. 3, but with added empirical frictional acceleration $a_f = 0.24v^2$.

is 0.31 m/s². It is reasonable that this value is much larger than that of constant rolling resistance because the average speed was 0.95 m/s, much larger than 0.5 m/s, and most importantly because the cylinder motion caused the ramp to shake, thus adding to the energy losses. A rolling resistance model with a constant value of a_f would not be sufficient to match the experimental data closely.

IV. OTHER MOTIONS

An interesting case occurs when the center of mass of the non-axisymmetric cylinder, after less than one complete revolution down the ramp, reaches the unstable equilibrium position for torque (vertically above the contact point) with zero velocity. Experimentally, this initial condition on ϕ , which we may call ϕ_{limit} , is the boundary between two very

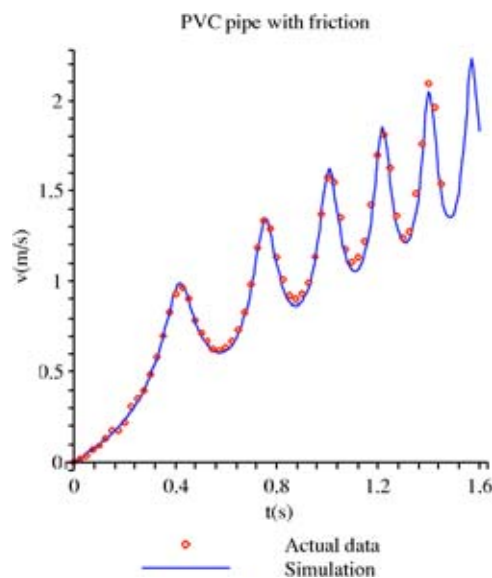


Fig. 5. PVC pipe. The following experimental values were used in the calculation: $\gamma = 9.7^\circ$, $\phi_0 = 180^\circ$, $m = 230$ g, $M = 255$ g, $R_2 = 4.4$ cm, $R_1 = 3.8$ cm, $R = 2.6$ cm, $r = 1.0$ cm, and $a_f = 0.1v$.

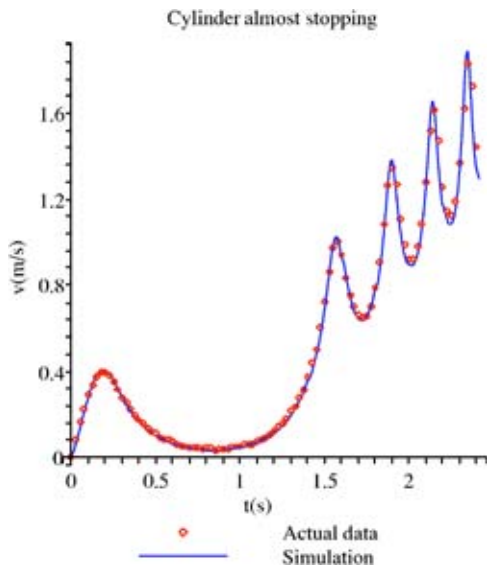


Fig. 6. PVC pipe released with M at $\phi_0=317^\circ$. The cylinder almost stops, then continues to roll as it accelerates down the ramp. A value of $a_f=0.0726v$ was used to match the experimental data.

different motions. A slightly smaller initial angle ϕ_0 will cause the cylinder to almost stop, but then resume speeding up as it moves down the ramp, whereas a slightly larger ϕ_0 will cause the cylinder to roll back up the ramp. The motion is thus very sensitive to the initial angle ϕ_0 . We tested the theory for motion starting with ϕ_0 near ϕ_{limit} and obtained reasonably good agreement with the data for both cylinders, slightly better for the PVC pipe can and $M \approx m$. With the PVC pipe, we could produce the first motion (slow down and resume) with $\phi_0=317^\circ$ and the second (roll back) with $\phi_0=318^\circ$. Both motions were reproduced closely by the calculation with the same values of ϕ_0 and with the assumption of a small amount of frictional acceleration $a_f \propto v$, as shown in Figs. 6 and 7. The initial angle ϕ_{limit} , determined experimen-

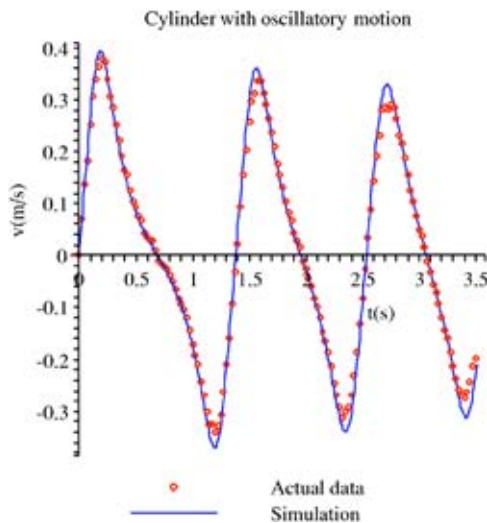


Fig. 7. PVC pipe released with M at $\phi_0=318^\circ$. The cylinder stops, rolls back up the ramp, and then continues in oscillatory motion. A value of $a_f=0.165v$ was used to match the experimental data.

tally to be $317.5 \pm 1^\circ$, can be obtained theoretically by equating the initial and final potential energy (neglecting frictional losses) as

$$\cos(\gamma + \phi_{\text{limit}}) + K\phi_{\text{limit}} = (\phi_{\text{equil}} + 2\pi)K - \sqrt{1 - K^2}, \quad (17)$$

where

$$K = \frac{R_2}{R_{\text{c.m.}}} \sin(\gamma), \quad (18)$$

and

$$\phi_{\text{equil}} = \frac{\pi}{2} - \gamma + \cos^{-1}(K). \quad (19)$$

A graphical solution of Eq. (17) gives $\phi_{\text{limit}}=318.7^\circ$, in good agreement with experiment. Note that small (but unaccounted) frictional losses would require an angle slightly smaller than the 318.7° predicted by the analysis, and thus the agreement is likely to be even closer. In the two cases considered in this section, the average absolute value of a_f was between 0.032 (oscillatory motion) and 0.04 m/s^2 , reasonably close to the constant rolling resistance value estimated to be 0.06 m/s^2 . This agreement is expected because the average speed in these cases was ≤ 0.5 m/s and other energy losses were negligible.

V. ENERGY CONSIDERATIONS

Information about the motion can be obtained by plotting T , T' , U , and E . For instance, we might expect that local minima of the potential energy function will occur when M is at the lowest point along the vertical, that is, at $\phi = -\gamma$, because past this point M starts rising inside the cylinder. However, $h_{\text{c.m.}}$ may still be decreasing if the motion is down a ramp. The minima of U can be located by setting $U' = 0$, which gives

$$\phi = -\gamma + \arcsin\left(\frac{R_2}{R_{\text{c.m.}}} \sin(\gamma)\right) + 2n\pi, \quad (20)$$

where n is an integer corresponding to the number of revolutions down the ramp. This condition forces $(R_{\text{c.m.}}/R_2)_{\text{min}} = \sin(\gamma)$. Otherwise, U will be a monotonically decreasing function with no local minima. For example, for the case in Fig. 5, Eq. (20) predicts minima at $\phi=23.06^\circ$. The numerical calculation produced local minima at $\phi=6.687, 12.970$, and 19.253 rad, corresponding to 23.1° after one, two, and three revolutions, respectively, in good agreement with the analytical formula.

VI. ADDITIONAL PROJECTS

We have presented a student project that can be tailored to meet a range of expectations and time frames, from a simple but nontrivial analytical solution to an extended project that requires the student to integrate analytical, computational, and experimental methods. To complete the project, the student is asked to derive equations for \ddot{x} , ϕ_{equil} , ϕ_{limit} , and the location of the minima of $U(\phi)$. Students need to build rigid asymmetric cylinders and an adjustable ramp free of vibrations, find ways to measure ϕ and γ accurately, determine whether slipping occurs, measure energy losses, align the

system carefully, and consider sources of error. In the following, we suggest some additional projects for more extensive challenges.

Give an alternate derivation of Eq. (16) starting from $T = T_{\text{cyl}} + T_M$ and $U = U_{\text{cyl}} + U_M$.

Find an alternative solution using $\dot{x} = f(x, p_x)$ and $\dot{p}_x = g(x, p_x)$, where $p_x = L \dot{x}$ and $\dot{p}_x = L \ddot{x}$.

Formulate a more accurate and thorough treatment of rolling resistance and other energy losses. For instance, the approach used here cannot match very closely all parts of the oscillatory motion on a horizontal surface if the motion lasts more than 10 s.

Show from geometry that there is a second equilibrium angle given by

$$\phi'_{\text{equil}} = \frac{\pi}{2} - \gamma - \cos^{-1} K. \quad (21)$$

Show that this angle is identical to that given by Eq. (20).

$$T = 2\pi \sqrt{\frac{MR^2 + (m+M)R_2^2 + \frac{m}{2}(R_1^2 + R_2^2) + M\frac{r^2}{2} - 2MRR_2 \cos(\phi'_{\text{equil}})}{MgR \cos(\gamma + \phi'_{\text{equil}})}}. \quad (23)$$

Compare this result to the output of the simulation and experiment. Note that in the simulation T actually varies slightly on the two sides ($\Delta\phi > 0$ and $\Delta\phi < 0$) of the oscillation around ϕ'_{equil} when the limits of applicability are tested, becoming shorter where U is steeper. This variation of T is not predicted by Eq. (23) because $\cos(\phi'_{\text{equil}})$ was used in place of $\cos(\phi'_{\text{equil}} + \Delta\phi)$.

Minimize slipping and energy losses due to vibrations for particularly jerky motions, for example, for large M or γ .

Devise a release method to accurately establish t_0 and v_0 . This is particularly relevant to matching theory and experiment for motions that start near an equilibrium point.

Investigate equilibrium and small amplitude oscillations about equilibrium. For $\gamma=0$ show that for small $\Delta\phi$ simple harmonic oscillations occur with period

$$T = 2\pi \sqrt{\frac{MR^2 + (m+M)R_2^2 + \frac{m}{2}(R_1^2 + R_2^2) + M\frac{r^2}{2} - 2MRR_2}{MgR}}. \quad (22)$$

Compare this result to the output of the simulation and experiment. For γ and $\Delta\phi$ small, where $\Delta\phi = \phi - \phi'_{\text{equil}}$, show that $U(\phi) = A\phi^2 - B\phi + C$ near ϕ'_{equil} , thus producing simple harmonic motion. The minimum of U occurs at $\phi = B/(2A)$, which again gives ϕ'_{equil} when γ is small. Show analytically that, for $\Delta\phi$ small and $R_{\text{c.m.}}/R_2 \geq \sin \gamma$, the equation for $\Delta\phi$ is exactly the equation for simple harmonic motion, and the period of oscillation is

ACKNOWLEDGMENT

The authors would like to thank the reviewers for their useful suggestions.

^{a)}Electronic mail: a.carnevali@moreheadstate.edu

^{b)}Electronic mail: r.may@moreheadstate.edu

¹H. Goldstein, *Classical Mechanics* (Addison-Wesley, Reading, MA, 1980), 2nd ed., p. 21.

²J. B. Marion and S. T. Thornton, *Classical Dynamics of Particles and Systems* (Harcourt Brace, New York, 1995), 4th ed, p. 241.

³Reference 2, p. 345.

⁴P. A. Tipler, *Physics* (Worth, New York, 1991), 3rd ed., p. 253.

⁵J. Y. Wong, *Theory of Ground Vehicles* (Wiley, New York, 1978), p. 13.

⁶B. L. Hannas and J. E. Goff, "Model of the 2003 tour de France," *Am. J. Phys.* **72**, 575–579 (2004).

⁷J. Witters and D. Duymelinch, "Rolling and sliding resistive forces on balls moving on a flat surface," *Am. J. Phys.* **54**, 80–83 (1986).